JOURNAL OF CATALYSIS **130**, 483–497 (1991)

Characterization of the Pore Structure and Morphology of Some Ion-Exchanged 12-Heteropoly Oxometalates

G. B. McGARVEY AND J. B. MOFFAT[1]

Department of Chemistry and Guelph–Waterloo Centre for Graduate Work in Chemistry, University of Waterloo, Waterloo, Ontario, Canada N2L 3G1

Received November 9, 1990; revised March 19, 1991

Monovalent 12-heteropoly oxometalate salts possessing the Keggin anion have been shown previously to undergo ion-exchange modification to various degrees such that the cation composition of the salts was altered. This study reports the results of investigations concerned with determining the effect of the ion-exchange procedure on the pore structure and morphology of the heteropoly salts. The analysis of nitrogen adsorption–desorption isotherms demonstrates that the ion-exchanged salts possess microporous structures. BET surface areas for the $K^+/NH_4^+/PW_{12}O_{40}$ and $K^+/NH_4^+/PMo_{12}O_{40}$ series of salts were found to undergo progressive changes as the cation composition was changed. Lattice parameters determined from powder X-ray patterns showed progressive changes as the cation composition was varied for each of the series of salts studied. The evidence suggests that the cation exchange occurs at sites within the microporous network of the 12-heteropoly salts. © 1991 Academic Press, Inc.

INTRODUCTION

In addition to compositional changes, it is well known that modification of solid-state materials using ion-exchange methods can lead to structural modifications of solids in general, and heterogeneous catalysts in particular (*1–4*). Ion-exchange methods have been used to advantage in several aspects of catalyst preparation including the modification of pore sizes and the incorporation or formation of reactive species in the catalyst structure.

The catalyst systems which have received the most attention as materials suitable for ion-exchange modification are the zeolites, particularly those possessing two- or three-dimensional channel pore systems. Exchangeable cations are often located at sites within the pores or cavities of the structure (*5*). Not all of the cation sites are equivalent, as their positions in cavities with openings of different pore size may preclude exchange with large cations. One consequence of cation exchange is the modification of the pore volume or pore diameter based entirely on the size of the exchanging cation. For example, the exchange of potassium ions for sodium ions in zeolite A reduces the adsorption pore size as a result of the increase in the cation diameter. Conversely, the pore size will increase following the exchange of calcium for sodium cations due to the decrease in cation density in the pore which results from the requirement of fewer divalent cations to achieve charge balance (*5*).

In addition to producing changes in the chemical composition and the resulting catalytic activity, ion exchange can be utilized as a method of modifying the secondary structure, or size and accessibility of the internal pores of many solid materials. This can serve not only to modify the active site distribution within the catalyst but also can place restrictions on the molecular species which enter or exit from the catalyst pores. It is well known that the cation present in zeolite A determines the range of pore volumes and pore sizes of the catalyst. Several other zeolites can undergo wide ranges of

---

[1] To whom correspondence should be addressed.

0021-9517/91 $3.00

internal pore modification which can result in variations in the ability of molecules to diffuse into and out of the pores. Indeed, several ion-exchanged zeolites are used in selective adsorption and sieving processes because the pore diameters can be tailored to the size required for a particular application. Dehydration of hydrocarbon streams is often carried out using the zeolite potassium A (or zeolite 3A), which possesses pores of approximately 3 Å that allow water to enter, but exclude the hydrocarbon molecules (*5b*). Zeolite calcium A or 5A has pore diameters of 5 Å, which allow linear alkanes to be separated efficiently from cyclic and branched species.

12-Heteropoly oxometalates are a family of materials which contain cations such as protons, alkali metal ions, and alkylammonium ions as a part of their structure. Several of these salts undergo ion-exchange reactions in a manner such that a limited number of the cations can be exchanged out of the solid phase (*6*). The extent of exchange has been found to be dependent on the nature of the cations that make up the exchanging pair and, specifically, on which cation of the pair is originally present in the solid phase. Significant differences were observed for exchange systems in which cesium was one of the cations. Whereas relatively large quantities of Cs^+ cations were exchanged into the NH_4^+ and K^+ salts of $H_3PW_{12}O_{40}$ and $H_3PMo_{12}O_{40}$, only small quantities of NH_4^+ and K^+ ions could be exchanged into the corresponding cesium salts.

The interest in microporous solids as potential catalysts for shape-selective reactions and the knowledge that some monovalent 12-heteropoly salts are microporous (*7–9*) were the impetus for the investigation of the pore structure of the ion-exchanged materials described in a previous paper (*6*). The presence of micropores and/or restricted pore openings can lead to selective formation of products because the reactant molecules may be too large to diffuse into the pores, the formation of certain transition-state species may be precluded based on molecular size or geometry, or the product molecules may not possess the proper geometry or size to diffuse out of the pore (*10*).

The measurement of adsorption isotherms or the sorption capacity of solid catalysts can yield information regarding the effect of ion exchange on the pore structure of the material. Changes in the surface area and pore volume will indicate that a change in the number of accessible sites may have taken place, and determination of pore radii and pore size distributions can lead to an a priori indication of the size of molecules that will be able to diffuse into the structure and which species may be excluded based on size considerations. Since the larger monovalent 12-heteropoly salts were found to be microporous (*7–9*), pore analysis of the exchanged materials can indicate whether the ion-exchange procedure was capable of effecting changes to the pore structure with the concomitant changes in the cation composition that occurred.

In addition to the differences in the pore structure, the secondary structure for the heteropoly salts was found to expand and contract as the size of the monovalent cation was increased or decreased, respectively (*7–9*). Therefore, powder X-ray diffraction techniques appear to be a valuable tool for investigating the structural type and the structural changes which result from the progressive incorporation of the cations in the ion-exchange procedure. Structural changes such as variations in the lattice parameters for the salts would provide strong evidence for the incorporation of the exchanging ions throughout the lattice, and not merely the sorption of the cations on the external surface of the solid through physical forces or weak electrostatic interactions.

The present investigation examines the effect of ion exchange of certain of the microporous heteropoly oxometalates on both the pore and crystallographic structures. For this purpose, nitrogen adsorption–desorption isotherms and powder X-ray diffraction patterns are obtained. The adsorption data were analyzed using several methods common to the characterization of porous materials, and such quantities as the surface area, micropore volume, micropore radii, and pore size distributions were determined. The results obtained from the powder X-ray diffraction patterns include determination of the lattice parameters and the intensity ratios for the [110] XRD reflection plane relative to the [222] plane, a quantity previously correlated with the micropore volume of 12-heteropoly oxometalate salts (*7–9*).

EXPERIMENTAL

The ion-exchanged salts used for this section of the research are those which were described in a previous publication (*6*). Ammonium tungstophosphate, $(NH_4)_3PW_{12}O_{40}$, ammonium molybdophosphate, $(NH_4)_3PMo_{12}O_{40}$, potassium tungstophosphate, $K_3PW_{12}O_{40}$, potassium molybdophosphate, $K_3PMo_{12}O_{40}$, cesium tungstophosphate, $Cs_3PW_{12}O_{40}$, and cesium molybdophosphate, $Cs_3PMo_{12}O_{40}$, were prepared from 12-tungstophosphoric acid and 12-molybdophosphoric acid by precipitation from aqueous solution using standard techniques. Following removal of the solvent, the salts were heated to 523 K for 3 h in air and subsequently cooled and stored in a desiccator. Each of the aforementioned salts was modified using ion-exchange methods with 0.1 *M* solutions of NH_4NO_3, KNO_3, and $CsNO_3$. Salts that were modified with cations different from that initially present in the solids were exchanged such that six samples were obtained. Each of the samples underwent a different number of ion-exchange reactions (up to six) allowing for the study of salts that had been subjected to various extents of exchange. The cation compositions (K^+, NH_4^+, Cs^+) of the ion-exchanged materials were determined using cation chromatography (*6*).

Nitrogen adsorption–desorption isotherms were measured using a volumetric glass vacuum system. The samples were outgassed at 10^{-5} Torr (760 Torr = 1 atm = 101.3 kPa) and 473 K for 2 h prior to measurement of the isotherms at 77 K. Gas chromatographic–mass spectrometric analyses of the gases released from the ammonium salts showed no evidence of the decomposition of the ammonium ions at this temperature.

TABLE 1

Cation Composition of the Ion-Exchanged 12-Heteropoly Salts

Ion-exchanged salt	M = Mo		M = W	
	Cation A	Cation B	Cation A	Cation B
NH_4PMNH_41	2.50	—	2.66	—
NH_4PMNH_42	2.47	—	2.66	—
NH_4PMNH_43	2.51	—	2.80	—
NH_4PMK1	1.99	0.60	2.27	0.79
NH_4PMK2	2.10	0.97	1.13	1.75
NH_4PMK3	1.44	1.23	1.45	1.35
NH_4PMCs1	1.75	1.15	1.41	1.14
NH_4PMCs2	1.42	1.41	1.26	1.46
NH_4PMCs3	1.30	1.53	1.18	1.44
$KPMNH_41$	1.67	1.00	1.86	0.39
$KPMNH_42$	1.50	1.12	1.29	1.53
$KPMNH_43$	1.36	1.37	0.67	2.01
$KPMK1$	3.03	—	3.04	—
$KPMK2$	3.02	—	2.96	—
$KPMK3$	2.90	—	2.99	—
$KPMCs1$	1.76	1.23	1.60	1.32
$KPMCs2$	1.58	1.45	1.47	1.46
$KPMCs3$	1.53	1.56	1.40	1.47
$CsPMNH_41$	2.59	0.04	2.73	0.19
$CsPMNH_42$	2.56	0.10	2.23	0.31
$CsPMNH_43$	2.44	0.14	2.49	0.38
$CsPMK1$	2.93	0.26	2.86	0.30
$CsPMK2$	2.94	0.30	2.69	0.42
$CsPMK3$	—	—	2.58	0.43
$CsPMCs1$	2.82	—	3.08	—
$CsPMCs2$	2.50	—	3.16	—
$CsPMCs3$	3.08	—	3.09	—

Powder X-ray diffraction patterns were recorded on a Siemens Model D500 diffractometer using nickel-filtered Cu*Kα* radiation. Patterns were recorded over the range $2\theta = 5–45°$. The samples were pretreated at 473 K for 2 h prior to the measurements and were supported in a sample holder with a depth of 1 mm.

RESULTS AND DISCUSSION

Surface Area and Pore Structure

Cation compositions of the salts for which nitrogen adsorption–desorption isotherms and powder XRD diffraction patterns were recorded are listed in Table 1. Positive devi-

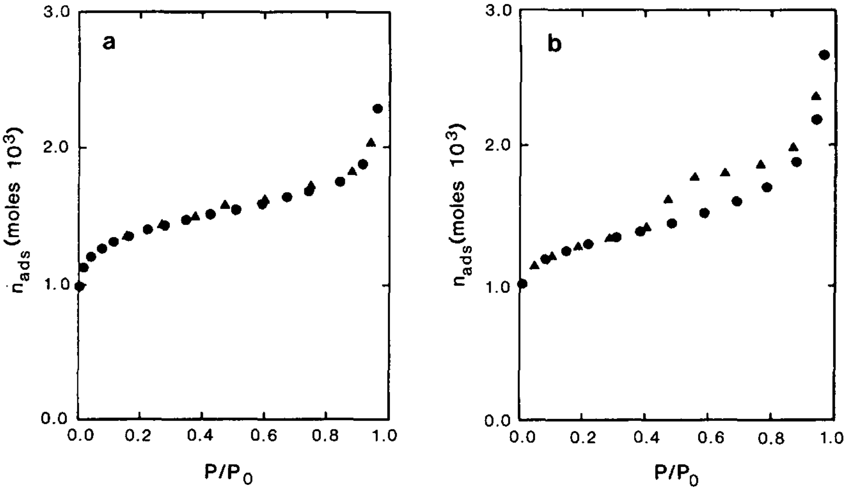

FIG. 1. Representative nitrogen adsorption–desorption isotherms for (a) $KPWNH_42$ and (b) NH_4PWK3.

ations from the stoichiometric value of 3 cations per anion are believed to result from experimental error in the analyses (<7%). In the cases where the number of cations is less than 3, it has been shown that the presence of protons accounts for a significant portion of the cations. Included in Table 1 is the notation that is employed to designate particular samples. The notation is *APMBn*, where *A* represents the cation present in the solid prior to the exchange modifications (one of K^+, NH_4^+, Cs^+), P*M* designates the anion (either PW for 12-tungstophosphate, $PW_{12}O_{40}^{-3}$, or PMo for 12-molybdophosphate, $PMo_{12}O_{40}^{-3}$), *B* represents the cation present in the liquid phase prior to the ion-exchange modification (one of K^+, NH_4^+, Cs^+), and *n* is a numeral used to distinguish between compositions for samples in the same exchange series. For samples with $n = 1$, the material has undergone one ion-exchange modification; for those with $n = 2$ the material has undergone three exchange modifications; and for $n = 3$ the material has undergone six ion-exchange reactions (five if the exchanging cation is the same as that initially in the salt). For example, sample CsPWK3 was prepared by exchanging solid $Cs_3PW_{12}O_{40}$ with 0.1 *M* KNO_3 six times, resulting in a material with a cation composition of 2.58 Cs^+ cations and 0.43 K^+ cations per $PW_{12}O_{40}^{-3}$ anion.

Representative nitrogen adsorption–desorption isotherms are shown in Fig. 1 for two of the mixed-composition heteropoly salts ($KPWNH_42$ and NH_4PWK3). In general, the isotherms for the high-surface-area salts displayed a sharp initial rise in the quantity of nitrogen adsorbed at low relative pressure of the adsorbate gas. As the relative pressure is increased throughout the intermediate pressure range, the quantity of nitrogen adsorbed from an aliquot of the gas decreased, although in the high-pressure region ($P/P_0 > 0.8$), some samples adsorbed large quantities of nitrogen. The large initial uptake of the adsorbate in the low-pressure region of the isotherm is often indicative of the presence of micropores in the solid. Several of the isotherms for the exchanged salts displayed hysteresis loops in the high-pressure region. This phenomenon is commonly associated with the presence of pores in the lower mesopore range (which is at the upper extremity of the micropore range). Interestingly, while most of the exchanged salts possessed isotherms with high initial uptakes of the adsorbate, the uptake for the KPMoCs2 and KPMoCs3 samples was quite small over the entire pressure range.

TABLE 2

BET Surface Areas and C_{BET} Parameters for the Ion-Exchanged 12-Heteropoly Salts

Ion-exchanged salt	M = Mo		M = W	
	S_{BET} ($m^2\ g^{-1}$)	C_{BET}	S_{BET} ($m^2\ g^{-1}$)	C_{BET}
$\mathrm{NH_4P}M\mathrm{NH_4}1$	88.0	1409	119.9	1643
$\mathrm{NH_4P}M\mathrm{NH_4}2$	80.5	877	137.7	1207
$\mathrm{NH_4P}M\mathrm{NH_4}3$	75.7	1136	134.2	643
$\mathrm{NH_4P}M\mathrm{K}1$	72.2	1252	131.2	996
$\mathrm{NH_4P}M\mathrm{K}2$	67.9	1098	119.5	1649
$\mathrm{NH_4P}M\mathrm{K}3$	56.8	1797	107.1	2795
$\mathrm{NH_4P}M\mathrm{Cs}1$	137.5	452	121.9	1301
$\mathrm{NH_4P}M\mathrm{Cs}2$	113.6	460	119.1	561
$\mathrm{NH_4P}M\mathrm{Cs}3$	85.7	376	116.3	651
$\mathrm{KP}M\mathrm{NH_4}1$	66.0	1896	122.7	1958
$\mathrm{KP}M\mathrm{NH_4}2$	60.8	2705	123.1	1880
$\mathrm{KP}M\mathrm{NH_4}3$	44.9	1739	126.4	2147
$\mathrm{KP}M\mathrm{K}1$	56.8	2203	110.9	1580
$\mathrm{KP}M\mathrm{K}2$	45.8	2131	104.2	3704
$\mathrm{KP}M\mathrm{K}3$	43.6	2674	100.6	2861
$\mathrm{KP}M\mathrm{Cs}1$	93.9	806	118.1	1539
$\mathrm{KP}M\mathrm{Cs}2$	21.7	93	121.0	1219
$\mathrm{KP}M\mathrm{Cs}3$	7.7	501	119.4	3638
$\mathrm{CsP}M\mathrm{NH_4}1$	110.1	472	131.1	524
$\mathrm{CsP}M\mathrm{NH_4}2$	71.9	194	124.3	493
$\mathrm{CsP}M\mathrm{NH_4}3$	60.2	177	114.6	611
$\mathrm{CsP}M\mathrm{K}1$	98.0	385	127.2	449
$\mathrm{CsP}M\mathrm{K}2$	44.3	150	117.3	467
$\mathrm{CsP}M\mathrm{K}3$	80.9	252	104.0	361
$\mathrm{CsP}M\mathrm{Cs}1$	88.5	205	127.6	636
$\mathrm{CsP}M\mathrm{Cs}2$	50.1	153	117.3	452
$\mathrm{CsP}M\mathrm{Cs}3$	41.3	181	108.4	1749

The surface areas of the salts were determined by using Brunauer/Emmett/Teller (BET) theory (*11*). Previous investigations of the adsorption of nitrogen on 12-heteropoly oxometalates have shown that the linear range of the BET isotherm is often greatly reduced for the microporous materials as compared to the non-porous materials (*7, 8*). BET plots for the ion-exchanged salts also varied greatly depending on the sample, and were restricted in linearity to the pressure range ~0.05–0.15 except for KPMoCs2 and KPMoCs3. Table 2 shows the surface areas calculated using the BET equation and the BET parameters (C_{BET}) for each of the ion-exchanged salts studied. It should be noted that the salts with surface areas greater than 40 $m^2\ g^{-1}$ showed higher initial uptakes of the adsorbate gas and reduced linear sections of their BET plots. The two samples which showed smaller uptakes of nitrogen were found to be low-surface-area materials for which the BET plots were linear over a wider pressure range.

Surface areas were also calculated using the method of Lecloux and Pirard (*12*) which entailed the construction of t-plots of the adsorption data from reference isotherms which were chosen based on the magnitude of the C_{BET} parameter. Results of the t-plot analyses for the ion-exchanged salts are listed in Tables 3 and 4. The agreement between the surface areas calculated using the two methods is quite good and provides confidence in the choice of the method of Lecloux and Pirard for construction of the t-plots from which the subsequent construction of pore size distributions is accomplished and mean micropore radii are calculated.

Figures 2 and 3 are plots of BET surface areas as a function of the cation composition (expressed as a mole percentage of the

TABLE 3

Micropore Analysis Data for 12-Tungstophosphate Ion-Exchanged Salts

Ion-exchanged salt	S_t ($m^2\ g^{-1}$)	V_{mp} ($cm^3\ g^{-1} \times 10^2$)	r_{mp} (Å)	n
$\mathrm{NH_4PWNH_4}1$	121.3	2.90	11.6	2.57
$\mathrm{NH_4PWNH_4}2$	138.5	2.75	12.3	2.55
$\mathrm{NH_4PWNH_4}3$	133.4	2.70	11.7	2.40
$\mathrm{NH_4PWK}1$	131.7	2.90	15.0	2.39
$\mathrm{NH_4PWK}2$	123.8	3.01	10.1	—
$\mathrm{NH_4PWK}3$	108.9	2.82	10.6	2.13
$\mathrm{NH_4PWCs}1$	120.5	2.89	11.3	2.55
$\mathrm{NH_4PWCs}2$	119.0	2.78	12.0	2.31
$\mathrm{NH_4PWCs}3$	116.8	2.98	11.7	2.48
$\mathrm{KPWNH_4}1$	124.8	1.86	7.63	2.28
$\mathrm{KPWNH_4}2$	123.8	3.00	10.5	2.20
$\mathrm{KPWNH_4}3$	124.8	3.13	10.9	2.32
KPWK1	111.6	2.66	11.4	2.30
KPWK2	104.9	2.78	9.41	2.18
KPWK3	101.4	2.55	10.4	2.15
KPWCs1	118.3	3.45	10.3	1.96
KPWCs2	120.9	3.33	10.1	1.93
KPWCs3	123.8	3.60	10.2	2.10
$\mathrm{CsPWNH_4}1$	128.9	1.78	—	2.97
$\mathrm{CsPWNH_4}2$	120.9	1.16	—	3.55
$\mathrm{CsPWNH_4}3$	114.6	1.93	—	3.30
CsPWK1	123.8	2.17	—	2.84
CsPWK2	114.6	0.77	—	3.26
CsPWK3	103.1	0.62	—	3.55
CsPWCs1	126.3	1.47	—	3.08
CsPWCs2	103.1	0.85	—	3.25
CsPWCs3	108.6	0.93	—	3.44

TABLE 4

Micropore Analysis Data for 12-Molybdophosphate Ion-Exchanged Salts

Compound	S_t (m^2 g^{-1})	V_{mp} (cm^3 g^{-1} × 10^2)	r_{mp} (Å)	n
NH_4PMoNH_41	89.7	1.58	10.77	2.65
NH_4PMoNH_42	81.4	1.58	11.99	2.46
NH_4PMoNH_43	76.2	1.50	10.86	2.51
NH_4PMoK1	72.5	1.62	12.06	2.50
NH_4PMoK2	67.3	1.55	10.35	2.24
NH_4PMoK3	57.3	1.61	9.54	2.01
$NH_4PMoCs1$	136.5	1.62	13.35	2.84
$NH_4PMoCs2$	114.6	1.16	14.20	3.14
$NH_4PMoCs3$	85.9	0.77	14.61	3.60
$KPMoNH_41$	66.3	1.52	8.70	2.33
$KPMoNH_42$	62.4	1.47	8.50	2.26
$KPMoNH_43$	44.2	1.08	9.10	2.29
KPMoK1	57.3	1.41	8.80	2.18
KPMoK2	47.6	1.24	8.75	2.10
KPMoK3	43.6	0.54	8.61	2.10
KPMoCs1	93.8	2.70	7.90	2.04
KPMoCs2	17.2	0.42	9.50	4.33
KPMoCs3	7.7	—	—	—
$CsPMoNH_41$	110.5	0.23	13.84	3.60
$CsPMoNH_42$	74.9	—	—	4.15
$CsPMoNH_43$	58.4	—	—	4.31
CsPMoK1	96.7	0.54	13.61	3.94
CsPMoK2	44.2	—	—	4.47
CsPMoK3	84.4	0.45	15.13	3.59
CsPMoCs1	88.4	0.39	14.90	4.10
CsPMoCs2	48.3	—	—	4.81
CsPMoCs3	42.2	—	—	4.77

total cation content) for the two series of salts, $K^+/NH_4^+/PW_{12}O_{40}^{-3}$ and $K^+/NH_4^+/PMo_{12}O_{40}^{-3}$. Regardless of which of the two anions is considered, the surface areas of the solids follow a decreasing trend as the cation makeup of the salts is changed from one in which ammonium is the predominant cation, through the intermediate compositions, to those for which potassium is the only cation present in the salt. Although there is scatter in the data, the overall trend toward changing surface area with cation composition can be seen quite readily, with the difference in surface area at the two extremes being approximately 40 m^2 g^{-1}. It should be noted that the surface area changes between the ammonium and potassium salts are consistent with a previous study that found that the ammonium salts possessed higher surface areas than the corresponding potassium salts for these two anions (*7*). The plots of surface area as a function of the cation composition are composites of data for two sets of exchanged salts. Each plot is composed of surface areas and cation compositions for salts prepared from the starting potassium and ammonium salts of each anion which had undergone exchange with the cation that was not originally present in the salt. The trend for both of these anion systems to display lower surface areas when the relative concentration of potassium ions is greater, regardless of which cation was initially present in the solid, suggests that the ion-exchange process for these systems is a bulk phenomenon

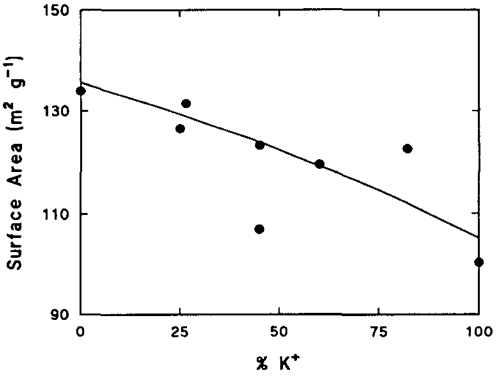

FIG. 2. BET surface area as a function of the cation composition for the ion-exchanged $K^+/NH_4^+/PW_{12}O_{40}^{-3}$ system.

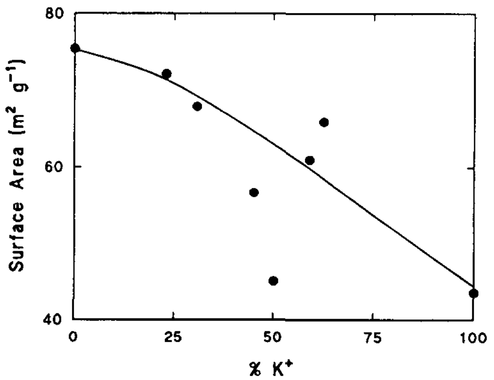

FIG. 3. BET surface area as a function of the cation composition for the ion-exchanged $K^+/NH_4^+/PMo_{12}O_{40}^{-3}$ system.

and is not restricted to the exposed or surface cations.

The t-plots for these salts were well behaved in that the extrapolated curves passed through the origin. A negative (downward) deviation in the plots was observed for the high-surface-area materials which contained K^+ and NH_4^+ cations, a phenomenon associated with the presence of micropores in the structure. In addition to the surface areas, the micropore volumes were estimated from the t-plots which displayed negative deviation as the thickness of the adsorbed layer increased. The micropore volume was estimated by extrapolating the t-plot curve from its linear section at high thickness values (or from the thickness equivalent to a relative pressure of $P/P_0 = 0.4$) to the ordinate and converting the intercept to a liquid volume. Tables 3 and 4 list the estimated micropore volumes for the ion-exchanged salts. The micropore volumes for the mixed-composition salts (K^+ and NH_4^+) of both of the anions studied remain quite constant regardless of the cation composition. Interestingly, for both series of salts, the magnitude of the micropore volumes for the exchanged salts more closely reflects the values obtained previously for the potassium salts than for the ammonium salts (*12*). It is also of interest to note that the micropore volumes for the $K^+/NH_4^+/PW_{12}O_{40}^{-3}$ series of salts are approximately twice those obtained for the corresponding $PMo_{12}O_{40}^{-3}$ salts.

Since no ab initio theory of adsorption in micropores is currently available, semiempirical techniques for the calculation of pore size distributions must be employed. The MP method is a procedure that has been developed to generate micropore size distributions from the data obtained from adsorption isotherms (*13*). Although the absolute accuracy of the method is subject to question, the values calculated have been shown to be internally self-consistent (*7*, *8*). Each of the K^+/NH_4^+ salts exhibited maxima in their pore size distributions in the micropore region. As can be seen in Figs. 4 and 5, no single size of micropore is present but instead distributions of pore sizes are evident. The $PW_{12}O_{40}^{-3}$ salts show a greater breadth in their distributions, with the maximum appearing in the region 8–10 Å, with evidence for pores up to 20 Å existing. The corresponding distributions for the $PMo_{12}O_{40}^{-3}$ salts are narrower, but show maxima in the same pore size region.

The pore size distributions did not change significantly with exchange for the KPWNH$_4n$ and KPMoNH$_4n$ series of materials. Larger changes were observed for the

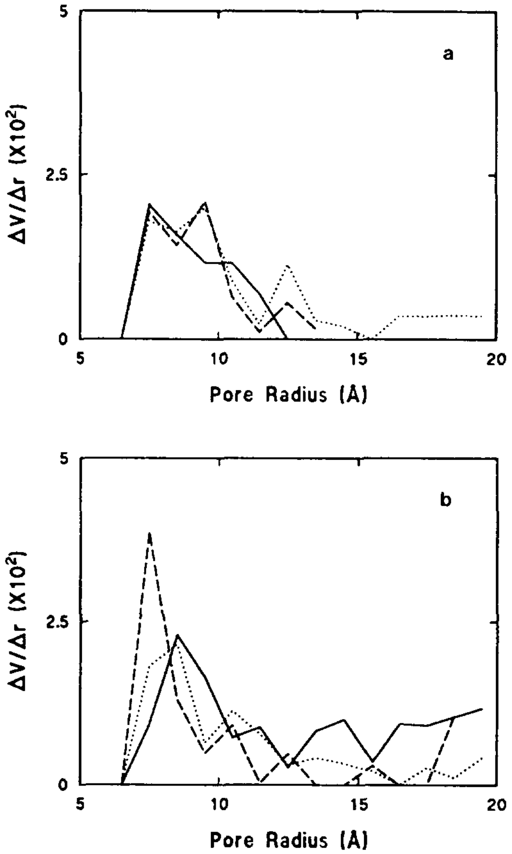

FIG. 4. Micropore size distributions for (a) $K_3PW_{12}O_{40}$ exchanged with 0.1 *M* NH_4NO_3 and (b) $(NH_4)PW_{12}O_{40}$ exchanged with 0.1 *M* KNO_3: —, one exchange reaction; ---, three exchange reactions; ···, six exchange reactions.

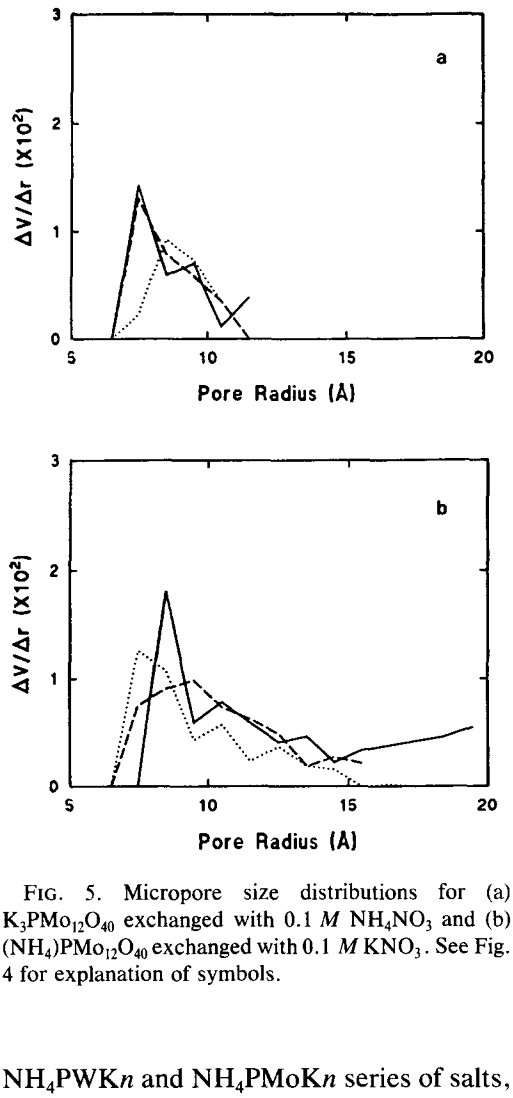

FIG. 5. Micropore size distributions for (a) $K_3PMo_{12}O_{40}$ exchanged with 0.1 *M* NH_4NO_3 and (b) $(NH_4)PMo_{12}O_{40}$ exchanged with 0.1 *M* KNO_3. See Fig. 4 for explanation of symbols.

NH_4PWKn and NH_4PMoKn series of salts, however. The changes in the breadth of these distributions and the location of the peak of maximum pore radius were found to depend to a greater extent on the ion-exchange number. For the NH_4PWKn series, the distribution passed through a maximum as the number of exchanges progressed from 1 to 6, while for the NH_4PMoKn series, there appeared to be a progressive change toward smaller radii as the number of exchanges increased. Pore size distributions do, however, confirm the retention of a microporous structure following the exchange modification.

Since distributions of pore sizes were evident for the ion-exchanged salts, mean micropore radii were determined for the materials that had pore size distributions in the micropore size range using the equation

$$\bar{r} = \frac{\sum(\Delta V/\Delta r)r}{\sum(\Delta V/\Delta r)}. \tag{1}$$

Tables 3 and 4 list the mean micropore radii for the exchanged salts. As the ammonium ions are exchanged into the potassium salts of both anions there is an increase in the mean micropore radius, while for the ammonium salt exchanged with potassium ions, the mean micropore radius is found to decrease as the number of potassium ions increases. These observations agree quite well with the published values for the mean micropore radii of K^+ and NH_4^+ salts which, for both anions, show that the potassium salt has a smaller mean micropore radius than the ammonium salt (*7*). While it can be argued that two different micropore distributions can yield the same mean radius, nevertheless, the result leads to a convenient single value for comparing the micropore size range of structurally similar catalysts.

Another quantity which can be used to assess the characteristics of pores is the number of adsorbed layers of the absorbate, *n*, which can be determined using the finite layer BET relationship

$$N = \frac{N_m C_{\mathrm{BET}} x[1 - (n + 1)x^n + nx^{n+1}]}{(1 - x)[1 + (C_{\mathrm{BET}} - 1)x - C_{\mathrm{BET}} x^{n+1}]} \tag{2}$$

where N_m and C_{BET} values were determined from the infinite layer relationship. By varying *n*, the number of adsorbed layers, theoretical values of *N*, the number of moles of nitrogen adsorbed, were calculated and compared with the experimentally determined quantities. A number of adsorbed layers of nitrogen less than 3 should correspond to the presence of micropores in the solid, while values of *n* greater than 3 indicate essentially free or unlimited adsorption on the surface with no restrictions imposed by

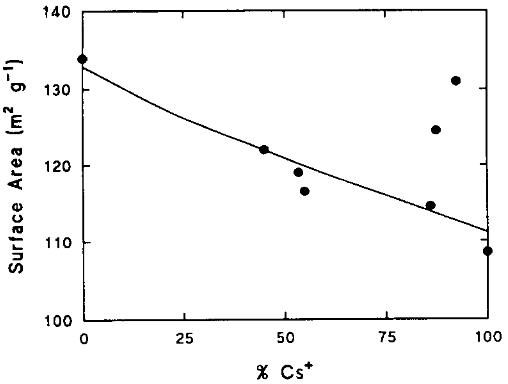

FIG. 6. BET surface area as a function of the cation composition for the ion-exchanged $NH_4^+/Cs^+/PW_{12}O_{40}^{-3}$ system.

the presence of pores. The K^+/NH_4^+ salts for each of the anions had *n* values generally less than 3, supplying further evidence for the presence of a microporous structure in these series of exchanged salts.

To this point, the discussion has dealt with the NH_4^+/K^+ exchange series of materials for each of the two anions. Analogous investigations of the NH_4^+/Cs^+ and K^+/Cs^+ series of ion exchanges were carried out to determine the effect of the ion-exchange modifications on the pore structure of these materials. Similar to the K^+/NH_4^+ series of salts, the adsorption isotherms for these salts displayed large initial uptakes of the adsorbate at low relative pressure. The exceptions were observed for KPMoCs2 and KPMoCs3 which showed very limited adsorption of nitrogen over the entire pressure range of the isotherms.

Unlike the NH_4^+/K^+ exchange systems, which displayed a correlation between the surface area and cation composition, the exchange systems which included Cs^+ as one of the exchange pair showed a larger degree of scatter when analogous plots were constructed (Fig. 6). The surface areas, BET parameters, micropore volumes, mean micropore radii, and number of adsorbed layers were determined and are listed in Tables 2–4. A possible explanation for the absence of apparent correlation between the surface area and cation composition is related to the large differences in the maximum exchange capacities within the series of salts depending on whether the Cs^+ ion is originally in the solid phase or in the liquid phase. The Cs^+ ion displays a strong tendency to replace NH_4^+ and K^+ ions that exist in the solid phase, while these two cations show only limited ability to exchange cesium cations from starting salts of either anion (*6*). Since the ion-exchange processes depend, at least in part, on the ionic radii of the cations and their ability to diffuse in and out of the microporous network, the aforementioned observations can be attributed to the effectively stronger binding energies for the larger Cs^+ ions than for the smaller K^+ and NH_4^+ ions. In addition, the exchanges that involve Cs^+ (in either the liquid or solid phase) approach the maximum degree of exchange after only two exchange reactions. K^+/NH_4^+ systems, on the other hand, progress through more gradual changes in the cation composition as the number of exchanges increases. The large discrepancy in the extent of exchange for the salts containing Cs^+ results in the clustering of points in two regions of the compositional spectrum. These regions are well removed from one another rather than evenly distributed across the cation composition range for the NH_4^+/K^+ points.

The surface areas for all of the cesium-containing salts were high (>40 $m^2\ g^{-1}$), except for KPMoCs2 and KPMoCs3, which suggests that these ion-exchanged salts were porous materials. Construction of the t-plots showed that, while all were well behaved and could be extrapolated through the origin, the shapes of the curves depended to a large extent on the cation pair and the cation of the pair which was originally present in the solid phase. The KPWCs, NH_4PWCs, and NH_4PMoCs salts had t-plots which showed the same downward deviation as the NH_4^+/K^+ series of salts, while those with Cs^+ cations originally present in the solid showed only a small degree of downward deviation. The t-plot surface areas were all in good agreement with those calculated using BET theory, again providing confidence in the choice of methods. Where the negative deviation of the t-plots was sufficient, micropore volumes were estimated and pore size distributions and mean micropore radii were determined (Tables 3 and 4).

Only seven of the samples which contained cesium (Tables 3 and 4) displayed t-plots which lacked the necessary curvature to estimate the micropore volume. Several samples however, lacked sufficient curvature to permit determination of micropore size distributions and, therefore, mean micropore radii. Each of the CsPWB salts had small micropore volumes, and micropore size distributions could not be determined. Similarly, several of the t-plots for various CsPMoB salts showed very little curvature and hence determinations of the pore size distributions and mean micropore radii were not possible.

Incorporation of Cs^+ ions into the NH_4PMo starting salt led to the formation of pores with mean radii that were approximately 2 Å larger than those for any of the other ion-exchanged salts with the $PMo_{12}O_{40}^{-3}$ anion. For the Cs^+-containing salts, the number of adsorbed layers was found to depend in large part on which cation of the exchange pair was originally present in the solid phase, or in other words, it depended on the ionic radius of the original cation. The number of adsorbed layers was generally found to increase as the radius of the cation A, for the general material APMB*n*, increased from K^+ to NH_4^+ to Cs^+. In particular, the number of adsorbed layers for the Cs^+ salts of each of the anions was significantly larger than for the corresponding K^+ and NH_4^+ salts. This is in accord with the smaller measured micropore volumes for these salts and the reduced amount of negative deviation in the t-plots for these materials, indicating that decreased quantities of micropores are present.

Surface areas, micropore volumes and related quantities were also determined for ion exchanged materials which were contacted with the same cation that was originally in the solid, i.e., CsPWCs*n*. The ion-exchange procedure did cause some changes in the surface areas of these materials as the number of exchanges increased. Exchange of the cation for residual protons which existed in the structure prior to the exchange procedure may at least partially account for such observations. It has been shown previously that the presence of protons in mixed-stoichiometry 12-heteropoly salts has an influence on the surface areas of these materials (*14*, *15*). The micropore volumes for the salts with only one cation are similar in magnitude to the volumes for salts with the same cation originally in the solid but with different cations from the liquid phase. Similarly, the number of adsorbed layers correlates with the increasing size of the cation in the solid since $K^+ < NH_4^+ < Cs^+$ for salts of both anions. Figure 7 is a plot of the mean micropore radius as a function of the number of adsorbed layers for the ion-exchanged

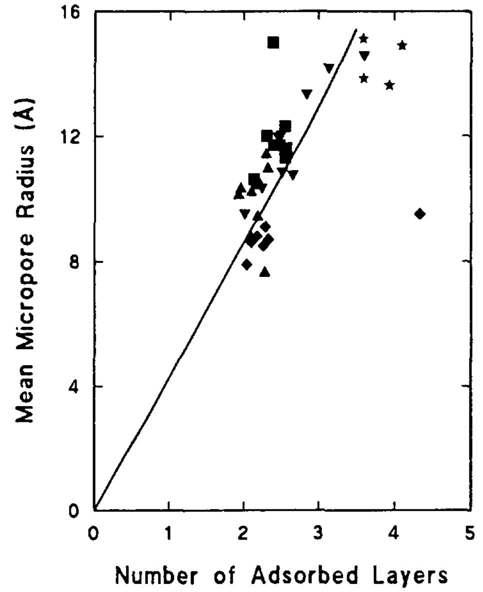

FIG. 7. Mean micropore radius as a function of the number of adsorbed layers for ion-exchanged 12-heteropoly salts: ◆, KPMo*Bn*; ▼, NH_4PMo*Bn*; ▲, KPW*Bn*; ■, NH_4PW*Bn*; ★, CsPMo*Bn*.

salts studied in this section. As expected a correlation exists between these quantities, as was observed for other monovalent 12-heteropoly salts that have been described previously (*9*).

It is worthwhile noting some qualitative aspects of the magnitudes of the C_{BET} parameters for the ion-exchanged salts. The C_{BET} parameter is related to the energy associated with the adsorption of the first monomolecular layer on the solid through the relationship

$$C_{BET} \approx \exp\left[\frac{E_1 - E_L}{RT}\right] \qquad (3)$$

where E_1 is the energy of adsorption of the first monomolecular layer and E_L is the energy of liquefaction of the adsorbate. If the adsorption energy for the formation of the first layer is high, as might be expected for adsorption in micropores where interactions with the walls will play a role, then the corresponding C_{BET} parameters will reflect this by being larger. In general, this is observed for the experimental results, although, not surprisingly, there is no direct correlation between the microporosity and the magnitude of the C_{BET} parameter.

It is evident that the presence of Cs^+ cations in the 12-heteropoly salts changes the pore structure significantly just as the ion-exchange behavior of the cesium salts was found to be much different than that for systems that included NH_4^+ and K^+ cations. Since the differences in ion-exchange behavior and pore structure of the heteropoly salts were found to depend so strongly on the cations included in the exchange pair, the structural changes that accompany the ion-exchange modifications were investigated by recording the powder X-ray diffraction patterns.

TABLE 5

Lattice Parameters and Intensity Data for the Ion-Exchanged 12-Heteropoly Salts

Ion-exchanged salt	M = Mo		M = W	
	a_0 (Å)	I_{110}/I_{222}	a_0 (Å)	I_{110}/I_{222}
$\mathrm{NH_4P}M\mathrm{NH_4}1$	11.648	0.478	11.643	0.481
$\mathrm{NH_4P}M\mathrm{NH_4}2$	11.649	0.444	11.640	0.410
$\mathrm{NH_4P}M\mathrm{NH_4}3$	11.647	0.538	11.648	0.390
$\mathrm{NH_4P}M\mathrm{K}1$	11.638	0.439	11.618	0.372
$\mathrm{NH_4P}M\mathrm{K}2$	11.625	0.458	11.610	0.353
$\mathrm{NH_4P}M\mathrm{K}3$	11.618	0.433	11.600	0.334
$\mathrm{NH_4P}M\mathrm{Cs}1$	11.679	0.330	11.716	0.344
$\mathrm{NH_4P}M\mathrm{Cs}2$	11.712	0.340	11.719	0.342
$\mathrm{NH_4P}M\mathrm{Cs}3$	11.716	0.288	11.722	0.284
$\mathrm{KP}M\mathrm{NH_4}1$	11.603	0.448	11.595	0.327
$\mathrm{KP}M\mathrm{NH_4}2$	11.615	0.456	11.606	0.257
$\mathrm{KP}M\mathrm{NH_4}3$	11.613	0.437	11.623	0.342
$\mathrm{KP}M\mathrm{K}1$	11.579	0.366	11.566	0.314
$\mathrm{KP}M\mathrm{K}2$	11.581	0.367	11.568	0.301
$\mathrm{KP}M\mathrm{K}3$	11.574	0.329	11.571	0.290
$\mathrm{KP}M\mathrm{Cs}1$	11.645	0.278	11.663	0.225
$\mathrm{KP}M\mathrm{Cs}2$	11.668	0.283	11.666	0.241
$\mathrm{KP}M\mathrm{Cs}3$	11.665	0.233	11.665	0.246
$\mathrm{CsP}M\mathrm{NH_4}1$	11.800	0.258	11.792	0.290
$\mathrm{CsP}M\mathrm{NH_4}2$	11.793	0.154	11.792	0.301
$\mathrm{CsP}M\mathrm{NH_4}3$	11.798	0.249	11.791	0.323
$\mathrm{CsP}M\mathrm{K}1$	11.784	0.231	—	—
$\mathrm{CsP}M\mathrm{K}2$	11.801	0.228	11.779	0.334
$\mathrm{CsP}M\mathrm{K}3$	11.705	0.354	11.719	0.344
$\mathrm{CsP}M\mathrm{Cs}1$	11.800	0.218	11.783	0.307
$\mathrm{CsP}M\mathrm{Cs}2$	11.802	0.220	11.803	0.325
$\mathrm{CsP}M\mathrm{Cs}3$	11.801	0.197	11.823	0.213

Structural Modifications Determined from Powder X-Ray Diffraction Measurements

Powder XRD patterns were recorded for the ion-exchanged salts for which nitrogen adsorption–desorption isotherms were measured. The diffraction patterns of the salts were all consistent with the cubic *Pn*3*m* space group that has previously been reported for 12-heteropoly salts (*7–9, 16–18*). The patterns were indexed and lattice parameters were calculated using the methods of Nelson and Riley (*19*). The a_0 values are listed in Table 5 for the different ion-exchanged salts.

The powder XRD patterns were consistent with the existence of a single crystallographic phase, in contrast to previous evidence for two distinct phases for a series of $K_{3-x}H_xPMo_{12}O_{40}$ salts (*14*). The present results undoubtedly demonstrate the importance that must be placed on the method of preparing monovalent 12-heteropoly salts. During the course of a precipitation (acid–base) reaction which is deficient in the number of cations sufficient to produce a stoichiometric compound, it may be expected that two distinct phases may be formed. This would appear to be the case, especially for systems that are significantly deficient in the number of cations since it has been reported that at least two of the large monovalent cations are necessary for the formation of an insoluble 12-heteropoly salt (*20*). In addition, crystallographic studies of ion-exchanged $K^+/NH_4^+/PMo_{12}O_{40}^{-3}$ salts have reported that only single crystallographic phases are present for the mixed cation salts (*21*). The crystals were shown to contain both K^+ and NH_4^+ cations, but only one lattice parameter was reported for each of the salts.

The materials considered in the present study display behavior that is more closely related to behavior of ion-exchanged salts from previous studies than to behavior of salts prepared by varying the initial ratio of cations and anions.

If the salts are divided into subsets on the basis of cationic and anionic compositions, some trends in the changes of a_0 are observed. For the series of salts APMB*n*, where A and M remain unchanged in chemical composition (but not necessarily in number) but B is changed from K^+ to NH_4^+ to Cs^+, the lattice parameter a_0 is found to increase with the radius of cation B; that is,

$$a_0(APMK) < a_0(APMNH_4) < a_0(APMCs). \quad (4)$$

The differences are particularly apparent for salts for which *A* is K^+ or NH_4^+, while for the series of salts for which *A* is Cs^+, there is much less difference in a_0 as *B* is changed from K^+ to NH_4^+ to Cs^+. As expected, the differences in the change in the lattice parameters are once again related to the extent of ion exchange or the maximum exchange capacity for the series. A lower exchange capacity (observed for the cesium salts of both anions) necessarily implies that fewer ions different from those originally present in the solid phase will be incorporated into the crystal structure of the exchanged salt. This implies that the lattice parameter will undergo less change in these materials than in salts where the exchange capacity is higher and the incorporation of cations of different radius will potentially affect the interanion spacing which in essence determines the value of a_0 while the size of the anion remains constant. The effect is particularly evident for KP*MB* and NH_4P*MB* salts for which a_0 differs by 0.03–0.04 Å as the cation radius for the cation being exchanged from the liquid phase into the solid phase increases.

Alternatively, the lattice parameters for salts with the same anion *M* and cation *B* can be considered as a subset, which considers and places emphasis on the cation that was originally present in the solid phase. Inspection of the data in Table 5 clearly shows that the cation present in the solid phase originally exerts the greatest influence on the magnitude of the lattice parameters. For a given cation *B*, a change of cation *A* from K^+ to NH_4^+ to Cs^+ results in an increase in the magnitude of a_0. For salts with the same *M* and *B* cations the difference in a_0 as *A* is changed from K^+ to NH_4^+ is approximately 0.04 Å, while the difference when *A* is changed from NH_4^+ to Cs^+ is approximately 0.1 Å. This reflects the fact that the difference between the ionic radii of K^+ and NH_4^+ is 0.1 Å and the difference between the ionic radii of NH_4^+ and Cs^+ is 0.24 Å (*22*). The differences in the lattice parameters are therefore one-half of the difference between the cation radii.

It is also interesting to consider the changes in the secondary structure of the ion-exchanged heteropoly salts as a function of the cation content of the materials. Figures 8–13 are plots of the lattice parameter as a function of cation composition for the three exchange series with the two different anions. The correlation for the change in lattice parameter is quite good for each of

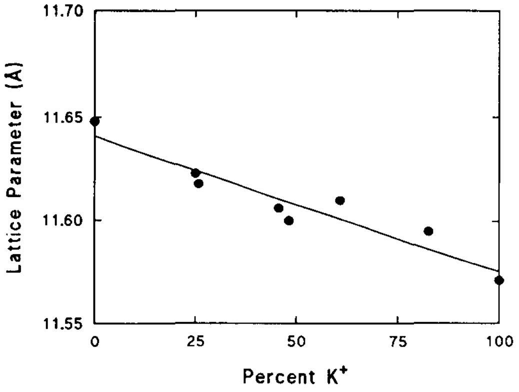

FIG. 8. Lattice parameter as a function of cation composition for the $K^+/NH_4^+/PW_{12}O_{40}^{-3}$ ion-exchange system.

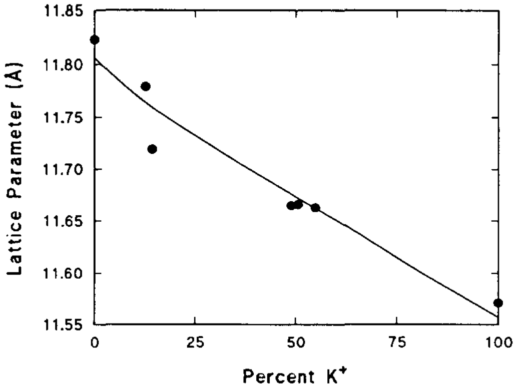

FIG. 10. Lattice parameter as a function of cation composition for the $Cs^+/K^-/PW_{12}O_{40}^{-3}$ ion-exchange system.

the exchange series. As was found for the changes in surface area, the systems which included K^+ and NH_4^+ as the two cations had a wider distribution of points across the entire composition range, resulting from the fact that the amount exchanged changed more gradually as the number of exchanges increased, with less evidence that the maximum exchange capacity was reached after the initial exchange. Those exchange series including Cs^+ with K^+ or NH_4^+ for either anion displayed clustering or grouping of the points on the plots of a_0 as a function of the cation composition. This results from the large differences in maximum exchange capacities depending on whether the Cs^+ ion is originally in the solid phase or in the liquid phase. The clustering is also related to the fact that the maximum exchange capacity is essentially reached following the initial exchange reaction. The absence of points across the complete composition range reduces the correlation somewhat, but the changes are still apparent for these systems.

Previous investigations of 12-heteropoly oxometalate salts have shown that salts which possess high surface areas and microporous structures also have intensity ratios

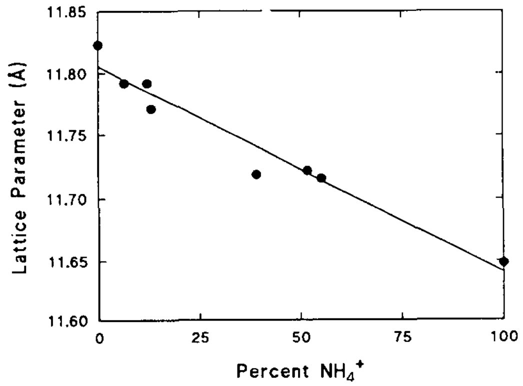

FIG. 9. Lattice parameter as a function of cation composition for the $Cs^+/NH_4^+/PW_{12}O_{40}^{-3}$ ion-exchange system.

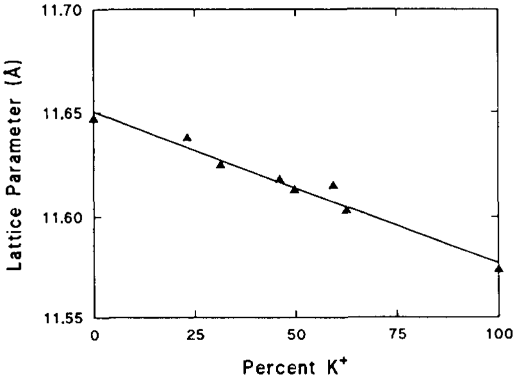

FIG. 11. Lattice parameter as a function of cation composition for the $K^+/NH_4^+/PMo_{12}O_{40}^{-3}$ ion-exchange system.

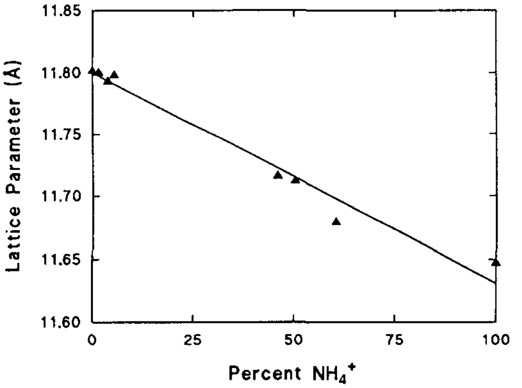

FIG. 12. Lattice parameter as a function of cation composition for the $Cs^+/NH_4^+/PMo_{12}O_{40}^{-3}$ ion-exchange system.

of the [110] XRD plane relative to that of the [222] XRD plane which are reduced from those for the parent acids and nonporous salts (*7–9*). The reduction in the intensity ratio is believed to result from the distortion of the terminal oxygen orientation as the larger cations (such as K^+, NH_4^+, and Cs^+) replace the proton and small cations. The ion-exchanged salts studied here, by virtue of the fact that they all contain the larger monovalent cations, all exhibited reduced intensity ratios (Table 5). These observations are in accord with the fact that the ion-exchanged salts were almost all high-surface-area materials, many of which contained significant microporosity.

There were no direct correlations observed between the I_{110}/I_{222} ratio and the surface area or micropore volume for the ion-exchanged salts, as had been observed for cases where a series of monovalent salts were prepared for a particular heteropoly anion (*7–9*). While this observation may at first seem incongruous with the previous results, it must be remembered that the range of intensity ratios for the microporous salts is relatively small when compared to the overall range of intensity ratios when all of the monovalent salts are considered (*7–9*). If the intensity ratios for these microporous salts of different cations are considered without considering those of the nonporous salts, it is once again found that there is no apparent correlation with the micropore volume. The results obtained with the ion-exchanged salts would therefore indicate that, while a reduced intensity ratio is required, it is not sufficient to ensure the existence of a microporous structure in the 12-heteropoly oxometalate salts.

The studies of pore structures and morphology have shown that ion-exchange modifications have brought about structural changes in the heteropoly salts. The exchange of cations into the secondary structure of the 12-heteropoly salts was found to be a bulk phenomenon from X-ray diffraction studies that showed definite changes in lattice parameters as the cation composition was progressively altered. The retention of high surface areas and significant microporosity indicates that the porous network was not destroyed or blocked as a result of the ion-exchanged modifications. This is an encouraging result in demonstrating that microporous 12-heteropoly oxometalate salts can be prepared and progressively modified without destroying the microporous structure that has been shown to be an enhancing factor for some catalytic processes.

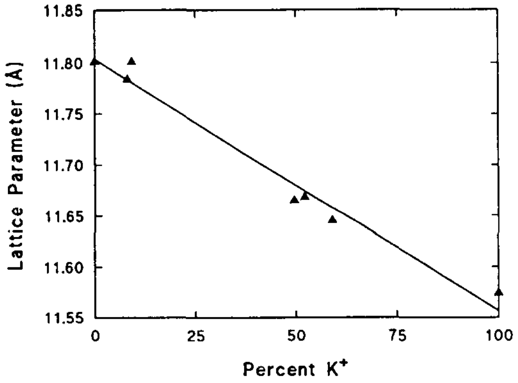

FIG. 13. Lattice parameter as a function of cation composition for the $Cs^+/K^+/PMo_{12}O_{40}^{-3}$ ion-exchange system.

SUMMARY

The ammonium, potassium, and cesium salts of 12-molybdophosphoric and 12-tungstophosphoric acids have been ion exchanged separately with each of the NH_4^+, K^+, and Cs^+ cations, the degree to which the exchange has occurred being altered by repeated and consecutive exchanges. Nitrogen adsorption–desorption and powder X-ray diffraction measurements on the ion-exchanged salts show that the microporosity and crystallography found in the unexchanged salts are retained, although, not surprisingly, the microporous structures and lattice parameters as well as the surface area are shifted on introduction of a second cation. The data for the salts with mixed cations appear to be reasonably self-consistent with those found for the corresponding single-cation salts. Although the microporous heteropoly oxometalates suffer from the disadvantage of possessing relatively broad pore size distributions, the catalytic merits of other microporous catalysts such as zeolites are expected to at least partly accrue to these catalysts. The demonstration in the present work of structure retention subsequent to ion exchange provides an incentive for further work on this topic, while the observations that the quantitative aspects of the structure are, for a given anion, controlled largely by the size and nature of the cation(s) open up the possibility of preparation of heteropoly oxometalates with predesigned structural properties.

ACKNOWLEDGMENTS

The financial support of the Natural Sciences and Engineering Research Council is gratefully appreciated. G.B.M. acknowledges NSERC and the Government of Ontario for financial support in the form of a postgraduate scholarship and Ontario Graduate Scholarship, respectively.

REFERENCES

1. Waller, F. J., *Catal. Rev. Sci. Eng.* **28,** 1 (1986).
2. Sherzer, J., *Catal. Rev. Sci. Eng.* **31,** 215 (1989).
3. Kerr, G. T., *Catal. Rev. Sci. Eng.* **23,** 281 (1981).
4. Rabo, J. A., *Catal. Rev. Sci. Eng.* **23,** 293 (1981).
5. Breck, D. W., "Zeolite Molecular Sieves," (*a*) p. 641, (*b*) p. 703. Wiley, New York, 1974.
6. McGarvey, G. B., and Moffat, J. B., *J. Catal.* **128,** 69 (1991).
7. McMonagle, J. B., and Moffat, J. B., *J. Colloid Interface Sci.* **101,** 479 (1984).
8. Taylor, D. B., McMonagle, J. B., and Moffat, J. B., *J. Colloid Interface Sci.* **108,** 278 (1985).
9. McGarvey, G. B., and Moffat, J. B., *J. Colloid Interface Sci.* **125,** 51 (1988).
10. Csicsery, S. M., *Pure Appl. Chem.* **58,** 841 (1986).
11. Brunauer, S., Emmett, P. H., and Teller, E., *J. Am. Chem. Soc.* **60,** 309 (1938).
12. Lecloux, A., and Pirard, J. P., *J. Colloid Interface Sci.* **70,** 265 (1979).
13. Mikhail, R. Sh., Brunauer, S., and Bodor, E. E., *J. Colloid Interface Sci.* **26,** 45 (1968).
14. Haeberle, T., and Emig, G., *Chem. Eng. Technol.* **11,** 392 (1988).
15. Black, J. B., Clayden, N. J., Gai, P. L., Scott, J. D., Serwicka, E. M., and Goodenough, J. B., *J. Catal.* **106,** 1 (1987).
16. Keggin, J. F., *Proc. R. Soc. A* **144,** 75 (1934).
17. Santos, J. A., *Proc. R. Soc. A* **150,** 309 (1935).
18. Brown, G. M., Noe Spirlet, M.-R., Busing, W. R., and Levy, H. A., *Acta Crystallogr. Sect. B* **33,** 1038 (1977).
19. Nuffield, E. W., "X-Ray Diffraction Methods," p. 157. Wiley, New York, 1966.
20. van R. Smit, J., and Robb, W., *J. Inorg. Nucl. Chem.* **26,** 509 (1964).
21. Boeyens, J. C. A., McDougal, G. J., and van R. Smit, J., *J. Solid State Chem.* **18,** 191 (1976).
22. "Handbook of Chemistry and Physics," 52nd ed., p. F171. CRC Press, Boca Raton, FL, 1972.